IJHSR
ijhighschoolresearch.org
RESEARCH ARTICLE

Optimization of a Vacuum-driven Origami Soft Robotic Gripper with a Combined Miura-ori Waterbomb Skeleton

Kai T. Unwin-Wisnosky

JP McCaskey High School, 445 N Reservoir St., Lancaster, PA, 17602, USA; 9898kaiw@gmail.com

ABSTRACT: Soft robotic grippers achieve robust and adaptive grasping performances through their flexibility. Creating substantial gripping strength across various object shapes and levels of fragility is a prominent challenge. This paper reports on experiments that tested whether a vacuum-driven origami soft robotic gripper with a novel combined Miura-ori Waterbomb skeleton pattern would increase gripping strength compared to a Waterbomb pattern. When gripping a sphere, a shape with a smooth and curved surface, and gripping a frustum, a shape with a wider bottom than top that is more difficult to grasp, across multiple pressures, the Miura-ori Waterbomb pattern demonstrated a significant increase in maximum gripping force. For both object shapes and all pressures, the Miura-ori Waterbomb pattern achieved maximum gripping strength at earlier extensions, demonstrating greater placement tolerance. These findings show that the soft gripper designed utilizing a combined Miura-ori Waterbomb skeleton pattern driven by negative pneumatic pressure (vacuum) produced significant increases in gripping strength and adaptability. This novel gripper design demonstrates potential across many applications in which gentle but strong grasping across varied object shapes is required.

KEYWORDS: Robotics, Robotic Kinematics, Soft Robotics, Origami, Vacuum, Gripper.

Introduction

Soft robots are robots that use compliant materials and designs to offer safer and more adaptive interactions with their environments and humans.[1,2] Traditional rigid robots create pressure points when gripping, require precise designs for certain manipulation tasks, and precise measurements and sensors for control. Soft robots, however, are able to handle a wide range of delicate, soft, and irregularly shaped objects with simplified control, as they distribute force across surfaces evenly, and inherent properties within them are able to account for uncertainty in placement and control.[3,4]

Adaptability is the ability to maintain gripping strength over diverse object shapes. By increasing adaptability, grippers can grasp wider ranges of objects, including heavier, fragile objects, without creating pressure points and minimizing potential damage. This broadens the potential applications for soft robotic grippers, including collaborative robotics (cobotics), where robots must safely interact with humans and account for error, marine and environmental sample collection, vessel cleaning, food harvesting, food packing, food waste reduction, and industrial part sorting.[5-11]

Pneumatically driven soft robotic grippers are one of the most common methods of actuation due to their simplicity, high performance, and low cost.[12] They are usually driven with compressed air, where applying positive pressure creates inflation and motion. However, their force production is greatly limited due to the material strength and the safety of applying positive pressure without bursting.[13,14] Alternatively, vacuum-driven soft robotic grippers apply a negative air pressure (vacuum) to drive implosion and contraction.[15] Although less explored, they pose many advantages. These include, firstly, increased safety and strength potential, as the actuator cannot burst because volume decreases on application of a vacuum, and secondly, increased ability to conform to diverse object shapes.[16]

A new type of vacuum-driven soft robotic actuator is Fluid-Driven Origami-Inspired Artificial Muscles (FOAM).[16] These use an origami pattern as a skeleton encased by an airtight, flexible thin skin. When a vacuum is applied, external pressure exceeds internal pressure, and the skin constricts the skeleton. This working principle is shown in the current experiment, Figure 1. This forces compression along the fold lines such that the kinematics of the actuator are controlled by the folding of the skeleton. Li *et al.*[17] demonstrated the practicality of a vacuum-driven soft robotic grasper using the FOAM principles and the "magic-ball" origami pattern. This pattern is an array of slightly offset waterbomb patterns that form a hemispherical shape with layers of gripping "teeth" and demonstrates a volume reduction of over 90% when contracted.[18,19] A folded example of the waterbomb "magic-ball" origami pattern is shown in the current experiment, Figure 2, right. Extension is the distance from the innermost point of the gripper cavity to the gripping object. At short extensions, the gripping object is deep inside the gripper cavity. At large extensions, the gripping object is close to the gripper opening. Li *et al.*[17] found that overall maximum gripping forces were at short extensions, yet for some object shapes, the gripper demonstrated a negative (pushing) force at those extensions, presenting a limitation in the adaptability of the design by Li *et al.* The current experiment introduces a novel combined Miura-ori Waterbomb pattern (Figure 2, left).

DOI: 10.36838/v8i1.34

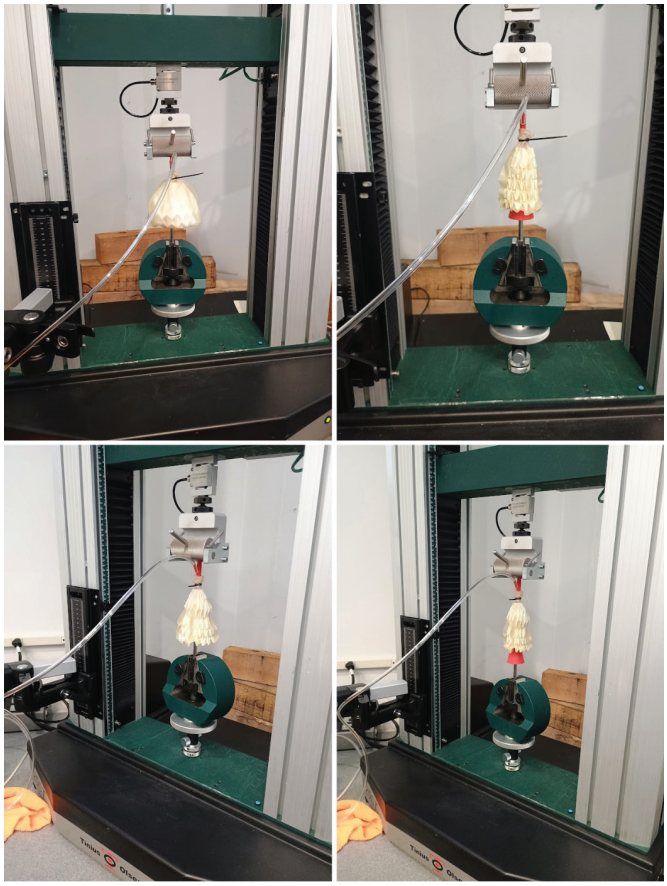

Figure 1: Miura-ori Waterbomb pattern Rest/Vacuum Off (bottom left); Miura-ori Waterbomb pattern Contracted/Vacuum On (bottom right); Waterbomb pattern Rest/Vacuum Off (top left); Waterbomb pattern Contracted/Vacuum On (top right); Working Principle: Vacuum makes external pressure exceed internal pressure, skin constricts the skeleton, folds along crease pattern, and gripper contracts around various shaped objects.

Figure 2: Folded Origami Skeletons; The combined Miura-ori Waterbomb pattern (left) consists of a Miura-ori upper portion and a Waterbomb "magic-ball" lower portion; The Waterbomb pattern (right) consists of a Waterbomb "magic-ball" pattern.

Vacuum-driven origami soft robotic grippers achieve their maximum gripping force at short extensions because there is a greater portion of the gripper exerting force, and the object is able to be fully enveloped by the gripper. When this occurs, lower portions of the skeleton are able to wrap around the object and create a mechanical lock underneath that contributes to greater gripping strength. While the waterbomb "magic-ball" pattern is able to achieve this mechanical lock, the pattern pushes objects out of the upper layers of teeth more easily because it contracts uniformly across the whole pattern, and the upper portion starts at a more contracted state. This is especially true for object shapes wider at the bottom than the top, such as the frustum, where the geometry of the object inherently creates a downward force.[17]

To address this in the current experiment, a novel pattern combining the Miura-ori and Waterbomb origami patterns was created. The Miura-ori pattern does not have the same volume-adapting properties, but instead has its own unique auxetic properties.[20] Materials with auxetic properties exhibit a negative Poisson ratio. Typical materials have a positive Poisson ratio: as they contract in the horizontal direction, they stretch in the vertical direction. In contrast, as a material with a negative Poisson ratio contracts in the horizontal direction, it contracts in the vertical direction. The combined Miura-ori Waterbomb pattern consists of a Miura-ori upper portion and a Waterbomb "magic-ball" lower portion (Figure 2, left). The auxetic properties of the upper portion, which exhibits less volume change, could contribute in two ways. First, by widening the upper portion, it could allow for larger objects to fit within. Second, it could create an additional force in the vertical direction that pulls objects into the upper layers of teeth. In combination, these traits could help to keep a wider range of objects enveloped in the upper layers, increasing gripping strength.

Research Question and Hypothesis:

The purpose of this experiment is to design, build, and determine which origami pattern yields more adaptive gripping: a combined Miura-ori Waterbomb pattern or a Waterbomb-only "magic-ball" pattern. Can changing the skeleton pattern of a vacuum-driven origami soft robotic gripper create more adaptive grasping, increased strength across multiple shapes?

The prediction was that the Miura-ori Waterbomb pattern would improve gripping strength and adaptability compared to the Waterbomb-only pattern. This was the prediction because of the auxetic properties of the Miura-ori pattern. While the uniform contraction of the Waterbomb "magic-ball" pattern partially pushes objects out of the top layers of gripping teeth, the Miura-ori maintains a wide upper portion that allows for larger objects to reach and be pulled into the upper layers of teeth upon contraction. This could increase the contraction force in the vertical direction as well as improve the mechanical lock in enveloping gripping objects.

■ Methods

Variables and Conditions:

The independent variable was the skeleton type (Combined Miura-ori Waterbomb vs. Waterbomb). The dependent variable was the gripping force produced (N). These variables were tested under the conditions of multiple vacuum pressures (-20 kPa, -30 kPa, -40 kPa, -50 kPa, and -60 kPa measured as gauge pressure) and multiple gripping object shapes (Sphere and Frustum). The controlled variables were the skeleton and skin mass and material, and gripper-object offset.

Design and Fabrication:

Vacuum-driven origami soft robotic grippers are made up of three components: the origami skeleton, the airtight skin, and the connecting centerpiece.

- ***Skeleton Fabrication:***

Origami skeletons were constructed using 176 g/m^2 (65lb) cardstock paper cut to be rectangles 47.2 by 14.75 cm and divided by folding into a 32 by 10 unit grid with unit length 1.475 cm (Table 1). A vertical 5 origami unit pattern was used to create a suitable internal volume and lower radius.[17] The crease pattern of each design seen in Figure 3 was scored by running the weight of a Stanley knife over the respective side valley folds to prepare creases for folding. The pattern was hand-folded, and ends were connected using Scotch Paper Tape on each side. The top layer was restricted to 2 cm using ZAP-A-GAP Medium CA+ Superglue.

Table 1: Table showing materials and specifications for each component.

Component	Material	Specifications
Skeleton	Cardstock Paper, 176 g/m^2 (65lb)	47.2 by 14.75 cm, folded into a 32 by 10 unit grid (1.475 cm unit length)
Skin	Clear Latex Rubber Balloons	24-inch, .25 mm thickness
Centerpiece	3D Printed ABS Plastic	2 cm diameter Circular Ridge
Gripping Objects	3D Printed ABS Plastic, .7 cm metal hex shaft	4 cm base diameter & height Frustum, 4 cm diameter Sphere, 13 g total weight each
Vacuum Pump	Preassembled	Pittsburgh Automotive 2.5 CPM Vacuum Pump
Vacuum Regulator	Preassembled	SMC Pneumatics IRV20 Vacuum Regulator
Tubing	Polyurethane Plastic	.25 in diameter
Load Tester	Preassembled	Tinius Olsen 25ST Universal Load Tester with 250N Load Cell, Horizon Software

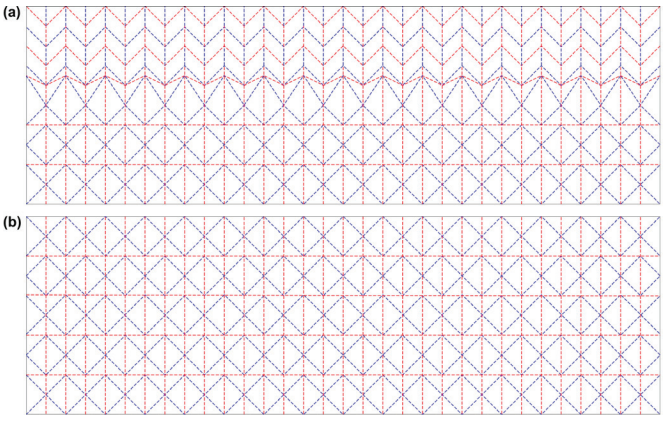

Figure 3: Origami Skeleton Crease Patterns; (a) Combined Miura-ori Waterbomb Pattern with a Miura-ori upper portion and a Waterbomb "magic-ball" lower portion; (b) Waterbomb Pattern with a Waterbomb "magic-ball" pattern.

Both the Miura-ori and Waterbomb patterns are rigidly foldable when considered individually.[21,22] However, when each is arranged into a hemispherical geometry for the soft robotic gripper, their folding is different: the Waterbomb pattern remains rigidly foldable, while the Miura-ori pattern requires slight bending of its parallelogram faces and is non-rigidly foldable. Due to the complexity of the non-rigid nature of the Miura-ori portion of the combined Miura-ori Waterbomb skeleton pattern, creating a 3D model using origami simulation software (Merlin II and Tesselatica) with thick panels for casting or 3D printing in silicone rubber was impractical within the time constraints.

An alternative skeleton material considered was polyethylene terephthalate film (PET), as it demonstrated effectiveness in research by Li *et al.*,[16,17] despite higher rigidity and less compliance than silicone. Crease patterns for both Miura-ori Waterbomb and Waterbomb patterns were laser cut from 10 mil PET using a Glowforge Pro laser cutter and hand folded (Figure 4, left). When tested, these grippers were non-functional: after contracting around an object, the patterns would deform and would not contract fully regardless of the pressure (Figure 4, right). This could be due to the combination of latex rubber skin material and PET, as the larger relative thickness and flexibility of the latex rubber could have caused skin constriction to drive fold extension (flattening) instead of fold compression. Additional experiments could investigate alternative skin materials and thicknesses relative to PET to enable contraction. Ultimately, cardstock was chosen as the skeleton material because of its memory-retaining properties similar to silicone.

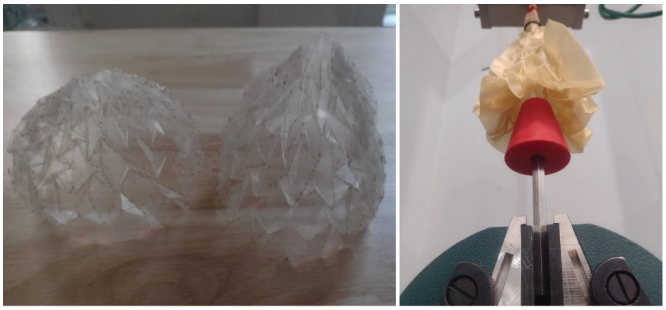

Figure 4: PET Waterbomb and Miura-ori Waterbomb Skeletons (left); PET Waterbomb Vacuum On During Testing (right); PET not chosen as skeleton material because grippers were not able to fully contract due to deformation.

- ***Vacuum Connection:***

A centerpiece was designed to connect the skeleton and skin to an external mount. The centerpiece consists of a circular ridge diameter of 2 cm at the base, to hook within the skeleton without impairing folding, a central indent, and airflow channels connecting the upper tube attachment point to the base ridge. The centerpiece was 3D printed in ABS Plastic. Small 1.5 cm Velcro squares were attached to the base of the centerpiece and inside 24-inch clear latex rubber balloons to ensure correct skin positioning. An airtight seal was formed between the centerpiece and skin using a rubber band wrapped around the indent and a zip tie to create a gasket and reduce air leakage (Figure 5).

DOI: 10.36838/v8i1.34

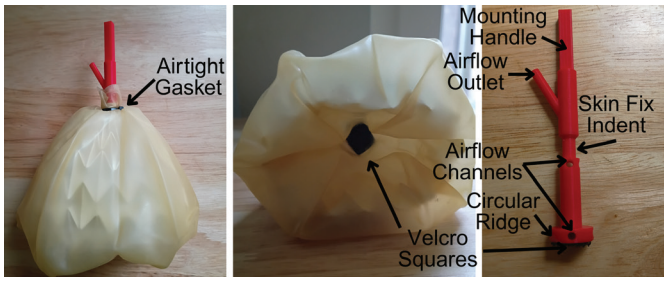

Figure 5: Vacuum Connection: Airtight gasket (left) connects skin and centerpiece; Velcro squares (center) maintain skin and centerpiece in correct position; 3D printed centerpiece (right) connects vacuum apparatus to skin, skeleton to gripper, and gripper to external mount.

- ***Object Construction:***

The gripping objects were 3D printed in ABS plastic with a 4 cm base diameter and height for the frustum, and a 4 cm diameter for the sphere, to fit in the first layer of gripper teeth. These were connected to 0.7 cm hex shafts. In total, each gripping object with the hex shaft weighed 13 g (Figure 6).

Figure 6: Gripping Objects: Sphere (left) and Frustum (right) connected to hex shafts to fix to Tinius Olsen 25 ST Universal Load Tester. A frustum shape with a wider base at the bottom than the top was tested to assess the combined Miura-ori Waterbomb pattern gripping adaptability improvements.

Experimental Procedures:

The airflow was connected between the Pittsburgh Automotive 2.5 CPM Vacuum Pump, SMC Pneumatics IRV20 Vacuum Regulator, and gripper centerpiece using 0.25 inch polyurethane plastic tubing (Figure 7). A 250N Load Cell was attached to the Tinius Olsen 25ST Universal Load Tester. The gripper centerpiece was positioned and tightened to be centered horizontally in the upper fixtures of the Load Tester. The gripping object hex-shaft was positioned and tightened to be centered horizontally in the lower fixtures of the Load Tester, in line with the gripper. The upper crosshead was lowered until the object was within, but not in contact with, the open gripper. The force reading was zeroed in the Horizon software. The upper crosshead was lowered at 50 mm/min until -1 N force was detected to ensure a consistent starting position. The Vacuum Pump was turned on, and the Vacuum Regulator was adjusted until the desired pressure was achieved. The upper crosshead was raised at 100 mm/min, and the load force was recorded until a 98% decrease from the maximum force reached, and the gripper released the object. The Vacuum Pump was turned off, and the Vacuum Regulator was adjusted to 0 kPa pressure.

The previous process was repeated for all vacuum pressures -20 kPa, -30 kPa, -40 kPa, -50 kPa, and -60 kPa, for both the combined Miura-ori Waterbomb and Waterbomb "magic-ball" skeletons, on both the Sphere and Frustum gripping objects. For each skeleton-object combination, three sets of trials were conducted using the same models, followed by three additional sets of trials with newly fabricated models. A total of 60 trials were conducted per skeleton design.

Trials were conducted in a randomized order across all pattern types, pressures, and gripping object shapes. Operator blinding was not required because the load tester was preprogrammed to automatically execute the testing sequence.

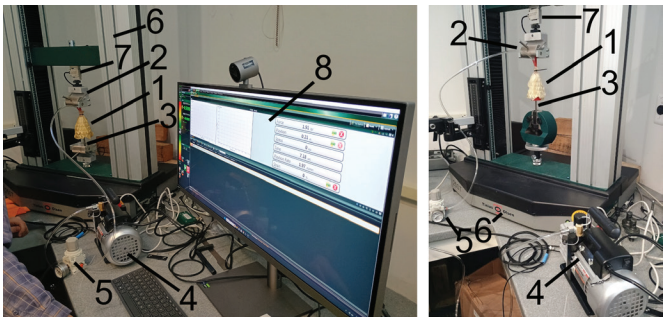

Figure 7: Load Testing Setup: Experimental Origami Soft Robotic Gripper (1) held in Upper Crosshead (2), Gripping Object (3), Vacuum Pump (4), Vacuum Regulator (5), and Tinius Olsen 25ST Universal Load Tester (6) with 250N Load Cell (7); Load Testing Setup with Horizon Force Data Analysis Software (8) (left); Load Testing Setup only (right).

Result and Discussion

The hypothesis was supported by the data in that, for both object shapes tested using a Tinius Olsen 25ST Universal Load Tester, across all pressures, the combined Miura-ori Waterbomb pattern produced a larger maximum gripping force than the Waterbomb pattern (Figure 8). When gripping a sphere, a shape with a smooth and curved surface, the Miura-ori Waterbomb pattern produced from a 21.7% (28.83 N to 35.1 N at -30 kPa) to 53.7% (44.75 N to 68.78 N at -60 kPa) increase in the maximum gripping force. When gripping a frustum, a shape with a wider bottom than top, the Miura-ori Waterbomb pattern produced from a 46.2% (40.18 N to 58.75 N at -30 kPa) to 71.9% (57.95 N to 99.63 N at -60 kPa) increase in the maximum gripping force. This demonstrates both increased adaptability and gripping strength across both shapes at equal pressures. In fact, at higher pressures, -50 kPa and above, the more adaptive pattern, Miura-ori Waterbomb, showed a maximum strength gripping the sphere shape, greater than the Waterbomb only pattern gripping a frustum shape. This demonstrates improved adaptability because the combined Miura-ori Waterbomb pattern was able to match and exceed the maximum gripping strength of the Waterbomb pattern for a different object.

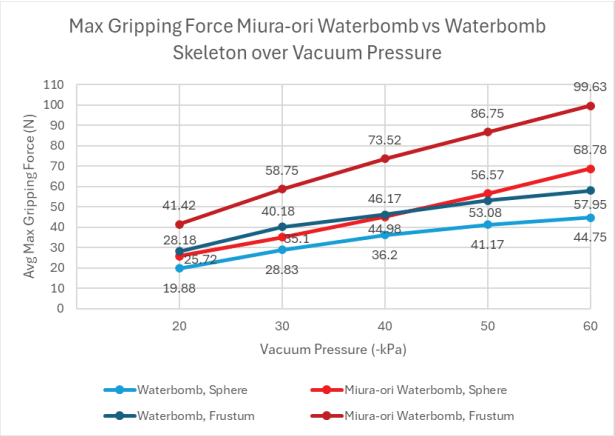

Figure 8: Across all pressures, the combined Miura-ori Waterbomb pattern produced a larger maximum gripping force than the Waterbomb pattern. When gripping a sphere, the Miura-ori Waterbomb pattern produced from a 21.7% (28.83 N to 35.1 N at -30 kPa) to 53.7% (44.75 N to 68.78 N) increase in the maximum gripping force. When gripping a frustum Miura-ori Waterbomb pattern produced from a 46.2% (40.18 N to 58.75 N at -30 kPa) to 71.9% (57.95 N to 99.63 N at -60 kPa) increase in the maximum gripping force. As vacuum pressure increases, the greater the increase in maximum gripping force of the Miura-ori Waterbomb pattern becomes. The combined Miura-ori Waterbomb pattern holds loads up to 99.63 N (22.4 lbs) at -60kpa. The linear relationship between vacuum pressure and maximum gripping force for both patterns indicates ease of gripping force control.

The Miura-ori Waterbomb pattern achieved a maximum gripping force of 99.63 N or 22.4 lbs when gripping a Frustum shape at a vacuum pressure of -60 kPa, while the Waterbomb pattern achieved a maximum gripping force of 57.95 N or 13.02 lbs under those same conditions (Figure 8).

Additionally, the Miura-ori Waterbomb pattern demonstrated improvements in gripping strength even at smaller pressures. For the smallest vacuum pressure tested, -20 kPa, for both a sphere and frustum shape, it produced a 29.9% and 47.0% increase, respectively, holding 25.72 N or 5.78 lbs and 41.42 N or 9.26 lbs. This demonstrates that the Miura-ori Waterbomb pattern is well-suited for heavier, fragile objects, where it is important to have a high gripping strength without creating pressure points that damage the object.

The results also show that as the vacuum pressure increases, the greater the increase in maximum gripping force of the Miura-ori Waterbomb pattern becomes. This indicates that the Miura-ori Waterbomb pattern should demonstrate improvements at even higher pressures than those tested, and could hold even heavier, fragile objects than the Waterbomb pattern.

An important aspect shared by the combined Miura-ori Waterbomb and Waterbomb patterns is the nature of their relationship between vacuum pressure and maximum gripping strength. Both patterns demonstrate a linear relationship, where vacuum pressure and maximum gripping strength increase at a constant rate. This indicates that it would be easy and straightforward to control the gripping force for the intended object. A simple ratio could be used to determine the output force based on vacuum pressure. This could be controlled with a flow regulator or adjustable electric power vacuum pump, using a feedback loop between either, and an internal pressure sensor to achieve a desired vacuum pressure, and through the ratio, output force.

The force (load) vs. extension graphs illustrate the structure of each gripper and the progression of the object being pulled from it (Figures 9 & 10). For all pressures and objects, the gripper reaches a peak force, followed by force drops corresponding to each layer of gripping teeth. For the Frustum, 3 distinct force drops are visible, aligning with the 3 tooth layers gripping in the waterbomb part of the pattern (Figure 9). For the sphere, these drops are also visible, although less distinctive due to the curved surface (Figure 10). This demonstrates how greater trends can be drawn from the force at each extension in the gripping process.

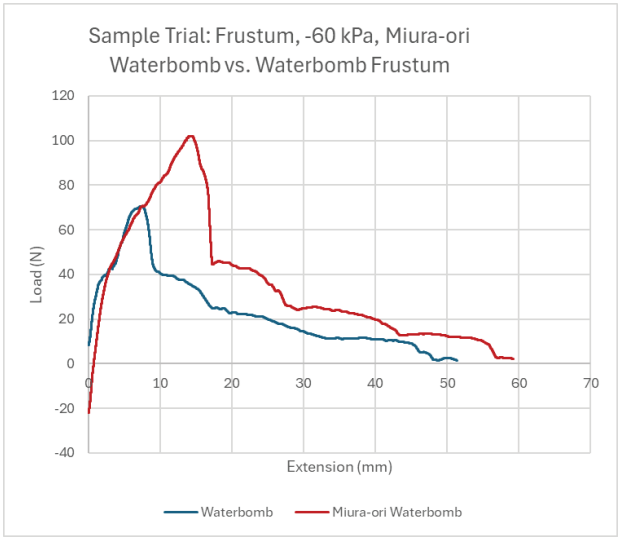

Figure 9: This shows the structure of Miura-ori Waterbomb and Waterbomb only skeletons as the Frustum is pulled from the gripper for a given trial (Trial 1). The gripper reaches a maximum force (load) at an early extension, followed by distinct force drops corresponding to each of the 3 following layers of gripping teeth. The Miura-ori Waterbomb pattern reaches a maximum force at a larger extension than the Waterbomb-only pattern. This allows for greater variation and levels of placement offset.

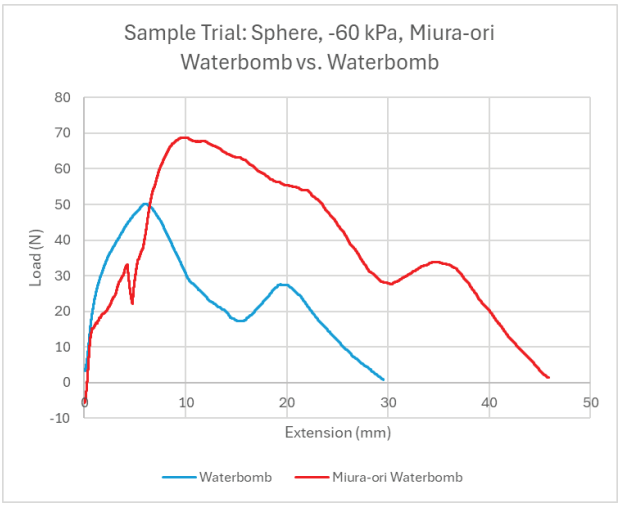

Figure 10: This shows the structure of Miura-ori Waterbomb and Waterbomb only skeletons as the Sphere is pulled from the gripper for a given trial (Trial 1). The gripper reaches a maximum force (load) at an early extension, followed by more gradual force drops than the Frustum as the Sphere goes through corresponding layers of gripping teeth. The Miura-ori Waterbomb pattern reaches a maximum force at a larger extension than the Waterbomb-only pattern. This allows for greater variation and levels of placement offset.

DOI: 10.36838/v8i1.34

An interesting difference between the Miura-ori Waterbomb and Waterbomb-only patterns is the extension at which the maximum gripping force is reached. For both object shapes and all pressures, the Miura-ori Waterbomb reached its maximum gripping strength at a larger extension (Figures 9 & 10). For the Frustum, it reached it at around 15 mm, and for the sphere, 10 mm, while the waterbomb reached it at 6 mm for both. This further illustrates the increased adaptability of the Miura-ori Waterbomb pattern, in that it allows for greater variation and levels of offset in placement while still achieving its maximum gripping strength. For soft and fragile objects, this would allow for more room for error in vertical placement, without risking bumping the object. For completely automated systems, it allows for increased irregularities in object size without this occurring. Additionally, human error is inherent in interaction and collaboration with robots in cobotics. The adaptability in vertical offset of the Miura-ori pattern demonstrates tolerance for this error, and paired with additional safety of soft-robots, has great potential application in this area.

The force (load) vs. extension graphs also demonstrate how object placement in the upper layers of teeth yields higher gripping strength. For both the Muira-ori Waterbomb and Waterbomb only patterns, the maximum gripping strength was achieved at relatively early extensions, with the above values over a total 60 mm extension (Figures 9 & 10). This confirms the idea that at these earlier extensions, the mechanical lock formed by completely enveloping the gripping object, in addition to a greater number of contact points, contributes to an increased gripping strength and shows that the prediction that the wider upper portion and auxetic properties of the Miura-ori would pull the object into the upper layers of the pattern and increase gripping force is correct.

The data for both Miura-ori Waterbomb and Waterbomb only patterns across all variations in pressure and object shape were analyzed using a p-value test (one-way ANOVA calculator with Tukey HSD *post-hoc*) to indicate statistically significant differences between group means and identify which pairs differed. This analysis found that for the majority of the trials, the p-value was less than .05, and therefore statistically significant (Table 2). However, it is shown that for the sphere at the vacuums -20, -30, and -40 kPa, the value was greater than .05. To help prevent possible deformation in the paper models across the trials, each set of origami skeletons was only used for 3 trials (all pressures, each object). However, individual variation in the hand folding and construction yielded differences in results for the same pattern. For the sphere at the lower vacuum levels, there is a clear difference between the maximum gripping force for trials 1-3 and 4-6. This shows that in the future, greater resiliency in the skeleton utilizing materials such as silicone might yield more consistent readings that could be tested across all 6 trials. This is not detrimental to the results, as when analyzed individually, each set of 3 trials still demonstrates the same conclusions as the overall data. Additionally, the frustum, which is more prone to a pushing force from gripping, had p-values all less than .05, showing that the most important results are all significant. The chart also shows that for the sphere, above -40 kPa, the values were significant. This indicates that at higher vacuum pressures, the intricacy of construction plays a less significant role in force production, as the force generated by pressure is proportional, while the variation from construction properties of the skeleton is constant.

Table 2: Table showing maximum gripping force for each trial, average maximum gripping force, standard deviation, 95% confidence intervals, and calculated p-values (one-way ANOVA calculator). P-values demonstrate statistical significance for frustum data at all vacuum pressures and for sphere data at -50 kPa and -60 kPa vacuum pressures. For the sphere at lower vacuum levels, there is a difference between the maximum gripping force for trials 1-3 and 4-6 due to new sets of origami skeletons every three trials to prevent deformation.

			Max Gripping Force (N)								
Gripping Object	Pressure (-kPa)	Skeleton Type	Trial 1	Trial 2	Trial 3	Trial 4	Trial 5	Trial 6	Average Max Gripping Force (Mean ± SD) (N)	95% Confidence Interval (N)	P-Values
Sphere	0	Waterbomb	0.0	0.00	0.00	0.00	0.00	0.00	0.00 ± 0.00	0.00 ± 0.00	
	0	Miura-ori Waterbomb	0.0	0.00	0.00	0.00	0.00	0.00	0.00 ± 0.00	0.00 ± 0.00	
	20	Waterbomb	25.00	26.00	29.00	12.30	12.80	13.30	19.88 ± 7.18	19.88 ± 5.75	0.15496
	20	Miura-ori Waterbomb	24.10	27.60	33.70	27.30	20.10	21.50	25.72 ± 4.50	25.72 ± 3.60	
	30	Waterbomb	33.70	34.90	36.20	23.60	22.00	22.60	28.83 ± 6.16	28.83 ± 4.93	0.16140
	30	Miura-ori Waterbomb	25.00	40.00	45.50	34.50	28.20	37.40	35.10 ± 6.92	35.10 ± 5.54	
	40	Waterbomb	41.20	40.90	40.90	33.70	30.40	30.10	36.20 ± 4.94	36.2 ± 3.95	0.07429
	40	Miura-ori Waterbomb	29.20	50.20	54.90	41.00	43.10	51.50	44.98 ± 8.53	44.98 ± 6.83	
	50	Waterbomb	45.80	45.40	46.30	37.70	35.30	36.50	41.17 ± 4.72	41.17 ± 3.78	0.00282
	50	Miura-ori Waterbomb	46.90	58.30	62.70	46.20	60.70	64.70	56.57 ± 7.38	56.57 ± 5.91	
	60	Waterbomb	49.00	50.20	49.00	37.30	41.40	41.60	44.75 ± 4.87	44.75 ± 3.90	0.000023
	60	Miura-ori Waterbomb	62.20	68.80	72.50	61.00	73.50	74.70	68.78 ± 5.40	68.78 ± 4.32	
Frustum	0	Waterbomb	0.00	0.00	0.00	0.00	0.00	0.00	0.00 ± 0.00	0.00 ± 0.00	
	0	Miura-ori Waterbomb	0.00	0.00	0.00	0.00	0.00	0.00	0.00 ± 0.00	0.00 ± 0.00	
	20	Waterbomb	32.20	41.00	32.20	22.90	21.60	19.20	28.18 ± 7.62	28.18 ± 6.10	0.016981
	20	Miura-ori Waterbomb	49.00	44.70	47.40	29.20	37.30	39.60	41.20 ± 6.75	41.20 ± 5.40	
	30	Waterbomb	46.10	52.80	41.90	37.30	32.70	30.30	40.18 ± 7.74	40.18 ± 6.19	0.001112
	30	Miura-ori Waterbomb	62.20	62.60	64.50	49.90	56.10	57.20	58.75 ± 4.96	58.75 ± 3.97	
	40	Waterbomb	55.70	47.40	51.50	45.40	40.00	37.00	46.17 ± 6.37	46.17 ± 5.10	0.00001
	40	Miura-ori Waterbomb	76.30	77.00	76.80	67.30	74.10	69.60	73.52 ± 3.76	73.52 ± 3.01	
	50	Waterbomb	62.90	56.90	58.40	50.90	45.50	43.90	53.08 ± 6.90	53.08 ± 5.52	0.00001
	50	Miura-ori Waterbomb	89.20	91.50	88.90	79.80	85.40	85.70	86.75 ± 3.75	86.75 ± 3.00	
	60	Waterbomb	70.50	61.90	62.90	55.20	49.20	48.00	57.95 ± 7.97	57.95 ± 6.37	0.00001
	60	Miura-ori Waterbomb	102.00	103.00	101.00	95.30	98.90	97.60	99.63 ± 2.65	99.63 ± 2.12	

Conclusion

In conclusion, a combined Miura-ori Waterbomb origami skeleton was developed that improved the gripping strength of a vacuum-driven soft robotic gripper across a variety of objects. This increased adaptability enables applications for soft and compliant gripping for relatively high loads in relation to its materials and weight. Applications include cobotics, marine and environmental manipulation for sample collection, vessel cleaning, food harvesting, food packing, food waste reduction, and industrial part sorting. The adaptable geometry of the origami pattern design and the interchangeable construction of other components could allow for cost-effective and rapid production of variations in design-based tasks. For example, further alterations to specific dimensions of the Miura-ori pattern could yield different negative Poisson ratios and further improve adaptability. Additionally, other origami pattern combinations could be tested to optimize for certain object types. Future experiments could test skeletons folded by scoring the crease pattern using a laser or robo-cutter to reduce hand-fold variations, and thus increase repeatability and further verify the significance of results. Skeleton materials such as silicone could be tested for greater resilience and flexibility. Skin materials with different stiffness levels or with adhesives could be tested to increase durability, consistency, and strength. Designs could also be tested across multiple sizes of grippers and objects to assess the scalability of the design. Combined control with both negative and positive pressure could be investigated for marine applications, where external water pressure at different depths could result in the gripper being contracted in its resting state. All of the above further testing could provide deeper insight into the adaptability and performance of a combined pattern origami soft robotic gripper.

Acknowledgments

Special thanks to Tinius Olsen Testing Machine Company for access to a Universal Load Tester.

References

1. Rus, D.; Tolley, M. T. Design, Fabrication and Control of Soft Robots. *Nature* **2015**, *521* (7553), 467–475. https://doi.org/10.1038/nature14543.
2. Kim, S.; Laschi, C.; Trimmer, B. Soft Robotics: A Bioinspired Evolution in Robotics. *Trends in Biotechnology* **2013**, *31* (5), 287–294. https://doi.org/10.1016/j.tibtech.2013.03.002.
3. Qaddoori Fenjan, S.; Fathollahi Dehkordi, S. Soft Robotic System with Continuum Manipulator and Compliant Gripper: Design, Fabrication, and Implementation. *Actuators* **2024**, *13* (8), 298. https://doi.org/10.3390/act13080298.
4. Andrius Dzedzickis; Jūratė Jolanta Petronienė; Sigitas Petkevičius; Vytautas Bučinskas. Soft Grippers in Robotics: Progress of Last 10 Years. *Machines* **2024**, *12* (12), 887–887. https://doi.org/10.3390/machines12120887.
5. Galloway, K. C.; Becker, K. P.; Phillips, B.; Kirby, J.; Licht, S.; Tchernov, D.; Wood, R. J.; Gruber, D. F. Soft Robotic Grippers for Biological Sampling on Deep Reefs. *Soft Robotics* **2016**, *3* (1), 23–33. https://doi.org/10.1089/soro.2015.0019.
6. Geckeler, C.; Mintchev, S. Bistable Helical Origami Gripper for Sensor Placement on Branches. *Advanced Intelligent Systems* **2022**, *4* (10), 2200087. https://doi.org/10.1002/aisy.202200087.
7. Hadi Ebrahimi Fakhari; Barboza, J. R.; Pezhman Mardanpour. Biomimetic Origami: A Biological Influence in Design. *Biomimetics* **2024**, *9* (10), 600–600. https://doi.org/10.3390/biomimetics9100600.
8. Kaufmann, J.; Bhovad, P.; Li, S. Harnessing the Multistability of Kresling Origami for Reconfigurable Articulation in Soft Robotic Arms. *Soft Robotics* **2021**. https://doi.org/10.1089/soro.2020.0075.
9. Laschi, C.; Mazzolai, B.; Cianchetti, M. Soft Robotics: Technologies and Systems Pushing the Boundaries of Robot Abilities. *Science Robotics* **2016**, *1* (1), eaah3690. https://doi.org/10.1126/scirobotics.aah3690.
10. Wang, X.; Khara, A.; Chen, C. A Soft Pneumatic Bistable Reinforced Actuator Bioinspired by Venus Flytrap with Enhanced Grasping Capability. *Bioinspiration & Biomimetics* **2020**, *15* (5), 056017. https://doi.org/10.1088/1748-3190/aba091.
11. Zhang, Y.; Quan, J.; Li, P.; Song, W.; Zhang, G.; Li, L.; Zhou, D. A Flytrap-Inspired Bistable Origami-Based Gripper for Rapid Active Debris Removal. *Advanced Intelligent Systems* **2023**, *5* (7). https://doi.org/10.1002/aisy.202370026.
12. Mosadegh, B.; Polygerinos, P.; Keplinger, C.; Wennstedt, S.; Shepherd, R. F.; Gupta, U.; Shim, J.; Bertoldi, K.; Walsh, C. J.; Whitesides, G. M. Pneumatic Networks for Soft Robotics That Actuate Rapidly. *Advanced Functional Materials* **2014**, *24* (15), 2163–2170. https://doi.org/10.1002/adfm.201303288.
13. Guo, J.; Sun, Y.; Liang, X.; Jin Huat Low; Yiik Diew Wong; Tay, V.; Chen-Hua Yeow. Design and Fabrication of a Pneumatic Soft Robotic Gripper for Delicate Surgical Manipulation. *IEEE Institute of Electrical and Electronics Engineers*, **2017**. https://doi.org/10.1109/icma.2017.8015965.
14. Gao, G.; Chang, C.-M.; Gerez, L.; Liarokapis, M. A Pneumatically Driven, Disposable, Soft Robotic Gripper Equipped with Multi-Stage, Retractable, Telescopic Fingers. *IEEE Transactions on Medical Robotics and Bionics* **2021**, *3* (3), 573–582. https://doi.org/10.1109/tmrb.2021.3097143.
15. Yang, D.; Verma, M. S.; So, J.-H.; Mosadegh, B.; Keplinger, C.; Lee, B.; Khashai, F.; Lossner, E.; Suo, Z.; Whitesides, G. M. Buckling Pneumatic Linear Actuators Inspired by Muscle. *Advanced Materials Technologies* **2016**, *1* (3), 1600055. https://doi.org/10.1002/admt.201600055.
16. Li, S.; Vogt, D. M.; Rus, D.; Wood, R. J. Fluid-Driven Origami-Inspired Artificial Muscles. *Proceedings of the National Academy of Sciences* **2017**, *114* (50), 13132–13137. https://doi.org/10.1073/pnas.1713450114.
17. Li, S.; Stampfli, J. J.; Xu, H. J.; Malkin, E.; Diaz, E. V.; Rus, D.; Wood, R. J. A Vacuum-Driven Origami "Magic-Ball" Soft Gripper. *IEEE International Conference on Robotics and Automation* **2019**.
18. Ma, J.; Feng, H.; Chen, Y.; Hou, D.; You, Z. Folding of Tubular Waterbomb. *Research* **2020**, *2020*, 1–8. https://doi.org/10.34133/2020/1735081.
19. Qiu, L.; He, Y.; Li, Y.; Yu, Y. Design and Parameter Optimization of a Biomimetic Jellyfish Origami Mechanism (BJOM) Based on Waterbomb Tessellations. *Mechanism and Machine Theory* **2023**, *184*, 105291–105291. https://doi.org/10.1016/j.mechmachtheory.2023.105291.
20. (1) Yu, M.; Yang, W.; Yu, Y.; Cheng, X.; Jiao, Z. A Crawling Soft Robot Driven by Pneumatic Foldable Actuators Based on Miura-Ori. *Actuators* **2020**, *9* (2), 26. https://doi.org/10.3390/act9020026.
21. Chen, Y.; Feng, H.; Ma, J.; Peng, R.; You, Z. Symmetric Waterbomb Origami. *Proceedings of the Royal Society A: Mathematical, Physical and Engineering Sciences* **2016**, *472* (2190), 20150846. https://doi.org/10.1098/rspa.2015.0846.
22. Yang, J.; You, Z. Cutting and Folding Thick-Panel Miura-Ori with One DoF. ASME International Design Engineering Technical Conferences and Computers and Information in Engineering Conference 2023. https://doi.org/10.1115/detc2023-112262.

Authors

Kai Unwin-Wisnosky is a JP McCaskey High School student in Lancaster, PA, USA. He plans to pursue mechanical engineering and conduct further research in origami engineering and energy technology. He hopes to continue applying creativity to engineering problem-solving for a better world.

DOI: 10.36838/v8i1.34